

Absorbing Boundary Conditions and Perfectly Matched Layers—An Analytic Time-Domain Performance Analysis

Adrianus T. de Hoop, Peter M. van den Berg, and Robert F. Remis

Abstract—The time-domain performance of a number of absorbing boundary conditions invoked on the boundary of a domain of computation, as well as of a perfectly matched layer surrounding such a domain, is carried out for a test configuration for which analytic expressions for the relevant field quantities exist. The test configuration consists of a small loop antenna radiating into a homogeneous, isotropic half-space. On the planar boundary of this half-space, either an absorbing boundary condition is invoked or a perfectly matched layer is started that is truncated at some finite depth of penetration. For a loop parallel to the boundary, closed-form analytic expressions for all field components of the spuriously reflected field are presented for all truncation conditions involved. A number of important features show up that might be masked in purely numerical implementations of the procedures under consideration.

Index Terms—Absorbing boundary conditions, computational modeling, perfectly matched layers.

I. INTRODUCTION

TRANSIENT-WAVE propagation and scattering problems are often analyzed in configurations of unbounded extent. The part of the configuration in which computational time-domain methods can be used to obtain the relevant field values is, however, necessarily of bounded support. This region, the *target region*, is taken to contain those parts of the configuration in which one is interested in the detailed behavior of the field quantities involved. The target region's *embedding* in \mathcal{R}^3 is, standardly, taken to have such simple physical properties that analytical representations can be constructed for the wave quantities in it. In principle, these representations can serve to construct boundary relations on the outer boundary of the target region that mimic the (passive) radiation into the embedding without affecting, as far as possible, the computed field values in the target region itself. Through the construction of the embedding's Green's function, the relevant boundary integral equations and Oseen's extinction theorem provide exact absorbing boundary conditions [1, Sec. 7.12, 15.12, and 28.12]. Both of these relations do yield interrelations between the field quantities, but they do so in a nonlocal and a noninstantaneous manner and, hence, ruin the computationally favored spatially band and

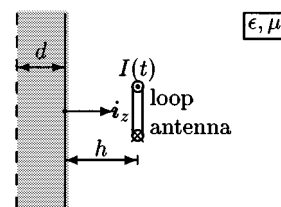


Fig. 1. Test configuration: radiating loop antenna with absorbing boundary conditions applied at $\{z = 0\}$ and perfectly matched layer in $\{z < 0\}$, truncated at $\{z = -d\}$.

explicit time structure of the algorithm (for example, the finite-difference time-domain one) for solving the relevant wave equations.

One way to preserve the computationally favored structure of the algorithm is to construct *absorbing boundary conditions* (ABCs) that sufficiently accurately approximate the exact boundary relations by spatially local and timely instantaneous ones. Several of these are known in the literature [2], [3]. More recently, truncated *perfectly matched layers* (PMLs), having absorption and/or time delay as their acting agents, have been introduced to serve the purpose [4]–[6]. The performance of both ABCs and PMLs is usually tested through purely numerical experiments. In such experiments, the employed signatures (pulse shapes) of the sources may hide some of the features that are inherent to the approximation at hand. The present contribution investigates the performance of a class of ABCs and a class of PMLs in a test configuration where analytic time-domain expressions for the field quantities are known and their features show up in all detail.

II. TEST CONFIGURATION

As a test configuration, we take an electric current carrying wire in the shape of a small planar loop that emits transient electromagnetic radiation into a homogeneous, isotropic medium with permittivity ϵ and permeability μ . The barycenter of the loop is located at $\{x = 0, y = 0, z = h > 0\}$, where $\{x, y, z\}$ are the coordinates with respect to an orthogonal, right-handed, Cartesian reference frame. The vectorial area of the loop is $\mathbf{A} = A\hat{z}$ (Fig. 1). Let $I = I(t)$ be the electric current in the loop, with t the time coordinate. Then, the electric field strength \mathbf{E} and the magnetic field strength \mathbf{H} of the emitted electromagnetic field are given by [1, Sec. 26.10]

$$\mathbf{E} = -\mu \partial_t \nabla \times \mathbf{F}, \quad \mathbf{H} = \nabla(\nabla \cdot \mathbf{F}) - c^{-2} \partial_t^2 \mathbf{F} \quad (1)$$

Manuscript received July 5, 2001.

The authors are with the Laboratory of Electromagnetic Research, Faculty of Information Technology and Systems, Delft University of Technology, 2628 CD Delft, The Netherlands (e-mail: a.t.dehoop@its.tudelft.nl; p.m.vandenberg@its.tudelft.nl; r.f.remis@its.tudelft.nl).

Publisher Item Identifier S 0018-9464(02)00952-4.

where $\mathbf{F} = F\mathbf{i}_z = (4\pi R_0)^{-1}AI(t - R_0/c)\mathbf{i}_z$ is the magnetic dipole vector potential, $AI(t)$ is the magnetic moment of the loop antenna, and $R_0 = [x^2 + y^2 + (z - h)^2]^{1/2} \geq 0$ is the distance from the barycenter of the loop to the point of observation.

III. WAVE-SLOWNESS FIELD REPRESENTATION

The construction of absorbing boundary conditions, and the terminology involved, standardly originate from the representation of the field expressed as a superposition of its wave slowness constituents parallel to the planar boundary on which the conditions are to be invoked. We shall illustrate the procedure for F . First, a one-sided, causal, time Laplace transformation is carried out. On the assumption that the exciting electric current is switched on at $t = 0$, the Laplace transform \hat{I} of I is given by

$$\hat{I}(s) = \int_{t=0}^{\infty} \exp(-st)I(t) dt \quad \text{with } s \in \mathcal{R}, s > 0. \quad (2)$$

We take the Laplace transform parameter s to be real and positive. (This implies that for the reconstruction of $I(t)$ from $\hat{I}(s)$ we have to rely on Lerch's uniqueness theorem [7, p. 63], since the standard Bromwich inversion integral would require complex values of s .) Correspondingly

$$\hat{F}(x, y, z, s) = \int_{t=0}^{\infty} \exp(-st)F(x, y, z, t) dt. \quad (3)$$

Subsequently, the wave slowness representation parallel to the plane $\{z = 0\}$ is written as

$$\hat{F}(x, y, z, s) = \left(\frac{s}{2\pi}\right)^2 \int_{\beta=-\infty}^{\infty} d\beta \int_{\alpha=-\infty}^{\infty} d\alpha \cdot \exp[-s(i\alpha x + i\beta y)] \tilde{F}(i\alpha, i\beta, z, s) \quad (4)$$

which entails the property $\tilde{\partial}_x = -si\alpha$, $\tilde{\partial}_y = -si\beta$. Since F satisfies the wave equation

$$(\partial_x^2 + \partial_y^2 + \partial_z^2 - c^{-2}\partial_t^2)F = -AI(t)\delta(x, y, z - h) \quad (5)$$

the slowness-domain equivalent \tilde{F} of F satisfies

$$(\partial_z^2 - s^2\gamma^2)\tilde{F} = -A\hat{I}(s)\delta(z - h) \quad (6)$$

in which $\gamma = (c^{-2} + \alpha^2 + \beta^2)^{1/2} > 0$ is the wave slowness normal to the plane $\{z = 0\}$. The solution is given by

$$\tilde{F} = \frac{A\hat{I}(s)}{2s\gamma} \exp[-s\gamma|z - h|]. \quad (7)$$

At the plane $\{z = 0\}$, we therefore have

$$\partial_z \tilde{F} = s\gamma \tilde{F} \quad \text{at } \{z = 0\} \quad \text{for all } \{\alpha, \beta\} \in \mathcal{R}^2. \quad (8)$$

This relation can be interpreted as characterizing the property that the half-space $\{z < 0\}$ totally, and exactly, absorbs the radiated field. As the expression for γ shows, the spatial counterpart of γ is a pseudo-differential operator that, due to its non-locality, destroys the sparseness of the finite-difference or finite-element discretization operators occurring in the computational field modeling.

TABLE I
ABSORBING BOUNDARY CONDITIONS

Type	α_N	α_D	Symbol
Taylor {0}	0	0	\square
Taylor {2}	1/2	0	∇
Padé {2,2}	3/4	1/4	\circ
Zero-crossing	1	0	\diamond
Zero-crossing Padé	1	1/2	*

To remedy this disadvantage, ABCs invoked as $z \downarrow 0$ or an extrapolation of the wave motion into a PML with support $\{-d < z < 0\}$ (i.e., one that is truncated at $\{z = -d\}$, where $d > 0$ is the thickness of the layer), are employed. For a class of ABCs and a class of PMLs exact space-time expressions for the spuriously reflected vector potential F^r in the half-space $\{z > 0\}$ will be determined in subsequent sections. From these, the corresponding electric and magnetic field strengths follow.

IV. ABSORBING BOUNDARY CONDITIONS (ABCs)

All ABCs replace (8) with the corresponding condition with γ replaced by some rational approximation γ^a in $i\alpha$ and $i\beta$ to γ about $\{\alpha, \beta\} = \{0, 0\}$. As the class of ABCs that we consider we take

$$\gamma^a = \frac{1}{c} \frac{1 + \alpha_N(\alpha^2 + \beta^2)c^2}{1 + \alpha_D(\alpha^2 + \beta^2)c^2} \quad (9)$$

in which the coefficients α_N and α_D are suitably chosen. For $\alpha_D = 0$ and $\alpha_N \neq 0$ the approximation is of the Taylor type, for $\alpha_D \neq 0$ and $\alpha_N \neq 0$ the approximation is of the Padé type (Table I). The corresponding boundary condition in space-time is

$$[c^{-2}\partial_t^2 - \alpha_D(\partial_x^2 + \partial_y^2)]\partial_z F = c^{-1}\partial_t [c^{-2}\partial_t^2 - \alpha_N(\partial_x^2 + \partial_y^2)]F \quad \text{as } z \downarrow 0. \quad (10)$$

V. SPURIOUSLY REFLECTED WAVE ABCs

Upon applying any of the ABCs of the type (9), the expression for the vector potential in the wave slowness domain becomes $\tilde{F} = \tilde{F}^i + \tilde{F}^{r;a}$, where \tilde{F}^i is given by the right-hand side of (7) and $\tilde{F}^{r;a}$ by

$$\tilde{F}^{r;a} = A\hat{I}(s)\tilde{R}^a \frac{\exp[-s\gamma(z + h)]}{2s\gamma}, \quad \text{for } z > 0 \quad (11)$$

in which the wave slowness domain reflection coefficient \tilde{R}^a follows as

$$\tilde{R}^a(\gamma, \gamma^a) = \frac{\gamma - \gamma^a}{\gamma + \gamma^a}. \quad (12)$$

Application of the first author's modification of the Cagniard method [8], [9] yields the following time-domain expression for $F^{r;a}$:

$$F^{r;a}(x, y, z, t) = AI(t) \overset{(t)}{*} \partial_t G^a(x, y, z, t) \quad (13)$$

in which $\overset{(t)}{*}$ denotes time convolution and

$$G^a(x, y, z, t) = \frac{R^a(x, y, z, t)}{4\pi R_1} \quad (14)$$

is the ABC Green's function. In the latter

$$R^a(x, y, z, t) = \left\{ \frac{2}{\pi} \int_{\psi=0}^{\pi/2} \operatorname{Re} \left[\tilde{R}^a(\bar{\gamma}, \bar{\gamma}^a) \right] d\psi \right\} H(t-T_1) \quad (15)$$

is the ABC time-domain reflection function, in whose expression $\bar{\gamma} = \bar{\gamma}(p, q)$ and $\bar{\gamma}^a = \bar{\gamma}^a(p, q)$ originate from $\gamma(i\alpha, i\beta)$ and $\gamma^a(i\alpha, i\beta)$, respectively, upon replacing $\alpha^2 + \beta^2$ by $q^2 - p^2$ and substituting

$$p = \frac{r}{R_1^2} t + i \frac{z+h}{R_1^2} (t^2 - T_1^2)^{1/2} \cos(\psi) \quad (16)$$

$$q = (t^2 - T_1^2)^{1/2} \sin(\psi). \quad (17)$$

Here, $r = (x^2 + y^2)^{1/2}$ is the offset of the point of observation from the normal to the boundary through the source, $R_1 = [r^2 + (z+h)^2]^{1/2}$ is the distance from the image of the source in the plane $\{z=0\}$ to the point of observation and $T_1 = R_1/c$ is the arrival time of the spuriously reflected wave. At $t = T_1$, the time-domain reflection function takes the value

$$R^a(x, y, z, T_1) = \frac{\bar{\gamma}(r/R_1 c, 0) - \bar{\gamma}^a(r/R_1 c, 0)}{\bar{\gamma}(r/R_1 c, 0) + \bar{\gamma}^a(r/R_1 c, 0)}. \quad (18)$$

VI. PERFECTLY MATCHED LAYERS

Next, the half-space $\{z < 0\}$ serves as a perfectly matched layer that we truncate at the plane $\{z = -d\}$, with $d > 0$. In this layer, the field equations that replace the exact ones are obtained by the transformations $\partial_x \rightarrow \partial_x$, $\partial_y \rightarrow \partial_y$, together with $\partial_z \rightarrow \chi_z(z, t)^{-1} \ast \partial_z$, and $\delta(x, y, z) \rightarrow \delta(x, y, z) \chi_z(z, t)^{-1} \ast$, where $\chi_z(z, t)$ is the time-domain equivalent of the causal, complex frequency-domain, z coordinate, *stretching function* of the layer [5], [6]. To comply with the condition that the differential equation in the stretched-coordinate domain admits causal solutions, it is assumed that $\hat{\chi}_z(z, s)$ is real and positive for real, positive values of s and all z . Under the stretching procedure, (6) is replaced by

$$\hat{\chi}_z^{-1} \partial_z \left[\hat{\chi}_z^{-1} \partial_z \tilde{F} \right] - s^2 \gamma^2 \tilde{F} = -A \hat{I}(s) \hat{\chi}_z^{-1} \delta(z-h). \quad (19)$$

The solution of this equation is

$$\tilde{F} = \frac{A \hat{I}(s)}{2s\gamma} \exp \left[-s\gamma \hat{Z}_0(z, h, s) \right] \quad (20)$$

in which

$$\hat{Z}_0(z, h, s) = \int_{\zeta=\min(z,h)}^{\max(z,h)} \hat{\chi}_z(\zeta, s) d\zeta \quad (21)$$

is the s domain PML stretched coordinate normal to the boundary. The corresponding time-domain expression for the unbounded medium follows from the inverse Laplace transformation of

$$\hat{F}^{i;\pi} = \frac{A \hat{I}(s)}{4\pi \hat{R}_0^\pi} \exp \left[-(s/c) \hat{R}_0^\pi \right] \quad (22)$$

in which

$$\hat{R}_0^\pi = \left[r^2 + \hat{Z}_0^2 \right]^{1/2}. \quad (23)$$

The truncation-generated reflected wave generated by invoking the boundary condition $F^{i;\pi} + F^{r;\pi} = 0$ as $z \downarrow -d$ (vanishing tangential electric field) follows as

$$\hat{F}^{r;\pi} = -\frac{A \hat{I}(s)}{4\pi \hat{R}_2^\pi} \exp \left[-(s/c) \hat{R}_2^\pi \right] \quad \text{for } z > -d \quad (24)$$

in which

$$\hat{R}_2^\pi = \left[r^2 + \hat{Z}_2^2 \right]^{1/2} \quad (25)$$

with

$$\hat{Z}_2(z, d, h, s) = \int_{\zeta=-(2d+h)}^z \hat{\chi}_z(\zeta, s) d\zeta \quad (26)$$

as the s domain PML stretched coordinate normal to the layer from the image of the source in the truncation plane $\{z = -d\}$ to the point of observation in the half-space $\{z \geq 0\}$. In this half-space, we have $\chi_z(z, t) = \delta(t)$, where $\delta(t)$ is the Dirac delta distribution. Consequently, in $\{z \geq 0\}$ the wavefield would remain undisturbed if the layer would not be truncated, as (20) indicates.

The class of PMLs whose performance we are going to analyze has profiles of the type

$$\hat{\chi}_z(z, s) = 1 + N(z) + s^{-1} \sigma(z) \quad (27)$$

where the PML *excess time delay profile* is given by

$$N(z) = \{A_N |z/d|^{\nu_N} \exp(-\beta_N |z+d|), 0\} \quad \text{for } \{-d < z < 0, z > 0\} \quad (28)$$

and the PML *excess absorptive profile* by

$$\sigma(z) = \{A_\sigma |z/d|^{\nu_\sigma} \exp(-\beta_\sigma |z+d|), 0\} \quad \text{for } \{-d < z < 0, z > 0\} \quad (29)$$

in which $A_N, \nu_N, \beta_N, A_\sigma, \nu_\sigma$, and β_σ are real-valued, nonnegative parameters. The corresponding total-field time-domain differential equation is

$$\begin{aligned} \partial_x^2 F + \partial_y^2 F + \chi_z^{-1}(z, t) \ast \partial_z \left[\chi_z^{-1}(z, t) \ast \partial_z F \right] - c^{-2} \partial_t^2 F \\ = -A \chi_z^{-1}(z, t) \ast I(t) \delta(x, y, z-h) \quad \text{for } z > -d \end{aligned} \quad (30)$$

in which

$$\begin{aligned} \chi_z^{-1}(z, t) = \frac{1}{1+N(z)} \delta(t) - \frac{\sigma(z)}{[1+N(z)]^2} \\ \cdot \exp \left[-\frac{\sigma(z)}{1+N(z)} t \right] H(t). \end{aligned} \quad (31)$$

VII. SPURIOUSLY REFLECTED WAVE PMLs

For the profiles (27)–(29), the spuriously reflected wave is

$$F^{r;\pi}(x, y, z, t) = -A I(t) \ast \partial_t G^\pi(x, y, z, t) \quad (32)$$

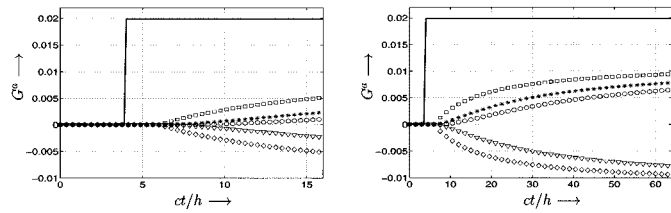


Fig. 2. ABC on-axis reflection: (left) early time and (right) late time.

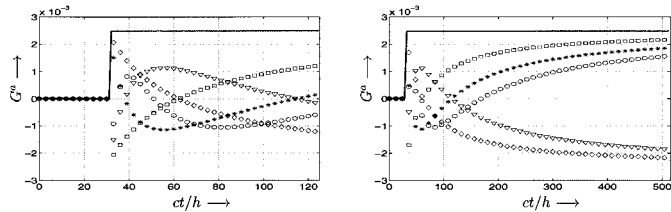


Fig. 3. ABC near-boundary reflection: (left) early time and (right) late time.

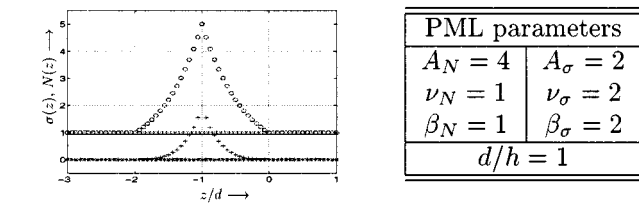


Fig. 4. PML excess time-delay and absorptive profiles.

in which

$$G^\pi(x, y, z, t) = \frac{\exp(-\Gamma t)}{4\pi R_2} J_0 \left[\Omega(t^2 - T_2^2)^{1/2} \right] H(t - T_2) \quad (33)$$

with J_0 the Bessel function of the first kind and order zero and

$$Z_2 = \int_{\zeta=-(2d+h)}^z [1 + N(\zeta)] d\zeta, \quad \Upsilon_2 = \int_{-(2d+h)}^z \sigma(\zeta) d\zeta. \quad (34)$$

$T_2 = R_2/c$, with $R_2 = (r^2 + Z_2^2)^{1/2}$, the travel time from the image source to the point of observation, $\Gamma = \Upsilon_2 Z_2 / R_2^2$ the damping coefficient and $\Omega = \Upsilon_2 r / R_2^2$ the angular frequency of oscillation.

VIII. NUMERICAL RESULTS

Figs. 2–6 show some ABC and PML numerical results in the form of time-domain wave waveforms of the relevant Green's functions G^a and G^π at 1) a location on the axis through the source ($r/h = 0$, $z/h = 5$) and 2) at a location near the boundary ($r/h = 32$, $z/h = 1$), emphasizing (left) early-time and (right) late-time behavior. The code indicating the type of ABC is given in Table I. The solid line marks the incident (i.e., desired) wave. The PML excess time-delay and excess absorption profiles are shown in Fig. 4. In all cases, the ideal situation would be the absence of a reflected wave. With an ABC,

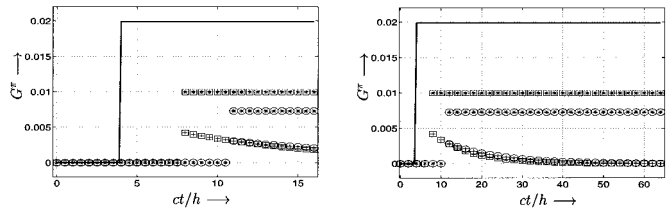


Fig. 5. PML on-axis reflection: (left) early time and (right) late time.

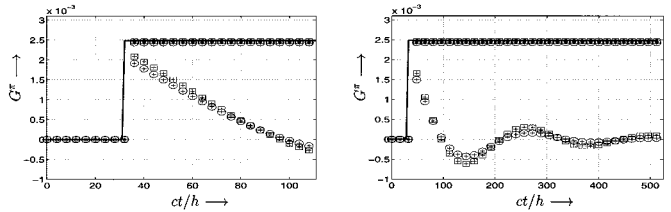


Fig. 6. PML near-boundary reflection: (left) early time and (right) late time.

early-time behavior on axis is superior to early-time behavior near the boundary. Late-time behavior of the reflected-wave Green's function is invariably dictated by the inverse distance amplitude decay only. A PML offers the advantage of steering the result through excess time delay and/or excess absorption in the layer. In a practical numerical simulation, the admissible profiles and their magnitudes are only restricted by the layer's thickness that one allows for in conjunction with the type of discretization stencil one employs. The input-source signature affects, as (13) and (32) show, via a convolution with the Green's function and a time differentiation the final result. Convolution is, however, a smoothing process whose final result may mask an inherently inaccurate Green's function. Because of the availability of analytic expressions, the present analysis does provide estimates of the performance of an ABC or a PML prior to its implementation in a finite-difference or finite-element code.

REFERENCES

- [1] A. T. de Hoop, *Handbook of Radiation and Scattering of Waves*. New York: Academic, 1995.
- [2] B. Enquist and A. Majda, "Absorbing boundary conditions for the numerical simulation of waves," *Math. Comput.*, vol. 32, pp. 629–651, 1977.
- [3] G. Mur, "Absorbing boundary conditions for the finite difference approximation of the time-domain electromagnetic-field equations," *IEEE Trans. Electromagn. Compat.*, vol. EMC-23, pp. 377–382, 1981.
- [4] J. P. Berenger, "A perfectly matched layer for the absorption of electromagnetic waves," *J. Comput. Phys.*, vol. 114, pp. 185–200, 1994.
- [5] W. C. Chew, W. M. Jin, and E. Michielssen, "Complex coordinate stretching as a generalized absorbing boundary condition," *Microw. Opt. Technol. Lett.*, vol. 15, pp. 599–604, 1997.
- [6] M. Kozuoglu and R. Mittra, "A systematic study of perfectly matched absorbers," in *Frontiers in Electromagnetics*, D. H. Werner and R. Mittra, Eds. New York: IEEE Press, 2000, ch. 14.
- [7] D. V. Widder, *The Laplace Transform*. Princeton, NJ: Princeton Univ. Press, 1946.
- [8] A. T. de Hoop, "A Modification of Cagniard's method for solving seismic pulse problems," *Appl. Sci. Res.*, vol. B8, pp. 349–356, 1960.
- [9] —, "Pulsed electromagnetic radiation from a line source in a two-media configuration," *Radio Sci.*, vol. 14, pp. 253–268, 1979.